

Demonstration of a High-Field Short-Period Superconducting Helical Undulator Suitable for Future TeV-Scale Linear Collider Positron Sources

D. J. Scott* and J. A. Clarke

*STFC Daresbury Laboratory, Daresbury, Warrington, Cheshire WA4 4AD, United Kingdom
and The Cockcroft Institute, Daresbury Laboratory, Warrington, Cheshire WA4 4AD, United Kingdom*

D. E. Baynham, V. Bayliss, T. Bradshaw, G. Burton, A. Brummitt, S. Carr, A. Lintern, J. Rochford, and O. Taylor

STFC Rutherford Appleton Laboratory, Chilton, Didcot, Oxfordshire OX11 0QX, United Kingdom

Y. Ivanyushenkov

Argonne National Laboratory, 9700 South Cass Avenue, Argonne, Illinois 60439, USA

(Received 1 April 2011; published 20 October 2011)

The first demonstration of a full-scale working undulator module suitable for future TeV-scale positron-electron linear collider positron sources is presented. Generating sufficient positrons is an important challenge for these colliders, and using polarized e^+ would enhance the machine's capabilities. In an undulator-based source polarized positrons are generated in a metallic target via pair production initiated by circularly polarized photons produced in a helical undulator. We show how the undulator design is developed by considering impedance effects on the electron beam, modeling and constructing short prototypes before the successful fabrication, and testing of a final module.

DOI: 10.1103/PhysRevLett.107.174803

PACS numbers: 41.75.Fr, 07.85.Qe, 85.70.Ay, 41.75.Ht

Future e^+e^- linear colliders such as the International Linear Collider (ILC) and Compact Linear Collider (CLIC) require $2.82 \times 10^{14} e^+ s^{-1}$, a factor of 60 increase of the most intense current sources such as the Stanford Linear Collider [1]. These *conventional* sources produce e^+ via pair production in a thick, $X_0 = 4.5$ radiation lengths, metallic target initiated by multi-MeV bremsstrahlung photons generated by a multi-GeV electron beam incident to the target. Extending this technology requires a 6.2 GeV, 253 kW electron beam, resulting in 48 and 142 kW being deposited in the target and downstream elements and target activation of 60 TBq leading to unsustainable thermal and radiation damage [2]. Additionally, conventional sources cannot produce polarized e^+ beams, which would increase the physics capability of the collider [3]. Polarized e^+ can be generated if the initial photon is circularly polarized as in the case of an undulator-based e^+ source (UBS), first described in 1979 [4]. Here, a multi-GeV electron beam passes through a helical undulator generating multi-MeV circularly polarized photons upstream of the target. Generating photons outside of the target gives two more advantages: thermal and radiation damage is significantly less, 7.2 and 5.85 kW to the target and downstream elements with target activation of 0.9 TBq [2], and the target can be thinner, $X_0 = 0.4$, resulting in less e^+ scattering and a factor of 3 increase in capture efficiency. A recent proof of principle experiment detected polarized e^+ generated in this manner [5,6]. Polarized e^+ beams can also be created via multi-MeV photons generated by scattering laser light off an electron beam [7,8]. These schemes rely on the development of high brightness electron beams, lasers,

and the alignment of multiple laser-electron interaction points; currently the photon intensity on the target is $\approx 10\%$ of that from the UBS and is not yet considered feasible for a collider. A UBS has been adopted by the ILC [9] and could be used for CLIC [10]. Until now the key component of the source design, a suitable helical undulator, had not been demonstrated. Previous work on the magnet technology choice [11] compared permanent magnet options against the well-known bifilar helix electromagnetic designs [12,13] and clearly demonstrated a superconducting (SC) bifilar helical winding design generated twice the on-axis field. A short model was built, achieving an on-axis field strength $B_0 = 0.81$ T with undulator period $\lambda_u = 14$ mm and free beam aperture $A_b = 4$ mm. The further studies presented here build on this early work by first selecting suitable undulator parameters that generate sufficient photon flux while having little impact on the electron beam quality and then fabricating a full-scale stand-alone SC helical undulator prototype that successfully demonstrates the specification, a vital step forward in proving the feasibility of future high intensity e^+ sources.

Optimizing a UBS is a multidimensional problem with many cross-talking parameters. For example, the electron beam energy, target material, thickness, capture efficiency, and damping ring (DR) acceptance all affect the source design. However, for any general parameter set, sufficiently increasing the undulator length increases the number of photons and hence the e^+ yield. For this reason a range of undulator parameters is possible; however, to minimize the undulator length a device with $B_0 \approx 1$ T,

$\lambda_u < 12$ mm, $A_b > 4$ mm, and operational safety margin is desirable [14]. The total length of undulator required is still ≈ 200 m even with these challenging parameters. The complete undulator would be built from shorter modules in a similar manner to planned and existing x-ray free-electron laser (FEL) undulators. The overall purpose of the complete undulator system is to generate sufficient 10 MeV photons, such that 3×10^{10} e^+ per bunch are captured in the DR. In addition, as the undulator uses the main collider electron beam, the beam quality, in terms of coherent energy spread σ_E and emittance ϵ , must not be degraded outside acceptable limits. These are affected by the impedance of the undulator vacuum vessel that has been modeled as a function of A_b in order to determine an acceptable specification. In turn this value for A_b determines the undulator minimum winding bore W_b via the vessel wall thickness: the vessel inner diameter is A_b and the outer diameter is W_b . Once W_b is established, magnet modeling is used to determine the minimum possible λ_u that generates 10 MeV photons with the first harmonic of the undulator.

Calculation of the impedances, explained in more detail in [15], were modeled by considering single bunch geometric and resistive wakefields (RW). A 150 GeV Gaussian ILC-type bunch with 10^{10} electrons and rms bunch length of 150 μm was modeled as the most demanding example. Typical frequencies in the bunch spectrum are 2 THz, which is similar in magnitude to the conduction electron collision frequency, and so ac conductivity models must be considered [16]. Ideally, electrical properties at the operating temperature of 4.2 K and at THz frequencies should be used; however, in this regime, the properties are highly dependent on the levels of impurities in the material and are difficult to assess. Therefore well-known reliable values available at 77 K have been used instead. The conductivity of the materials considered is known to increase as the temperature decreases, so using these intermediate temperature values will predict an overly pessimistic RW effect. Experiments are planned to measure the electrical properties of typical vessels in the required regime [17]. Also, the anomalous skin effect conductivity model must be used [18]. This model is suitable when the skin depth δ is small compared to the mean free path λ_F of the conduction electrons; for example, at 2 THz in copper at 77 K, $\lambda_F = 330$ nm and $\delta = 40$ nm. These results show that, for $4 < A_b < 6$ mm, the longitudinal RW W_{\parallel} from a stainless steel vessel would induce $1.3\% < \sigma_E < 1.9\%$, which is too great. Similar copper, gold, and aluminum vessels would induce only $0.09\% < \sigma_E < 0.17\%$, which is acceptable. The vessel surface roughness R_a should not increase σ_E by $\approx 10\%$. Using a pessimistic inductive impedance model of R_a [19], a vessel with $4 < A_b < 6$ mm would require $R_a < 300$ nm. A survey of available narrow aperture off-the-shelf vessels established that only a copper vessel was able to meet the smoothness and material specification.

The selected vessel has $A_b = 5.85$ mm, $R_a = 125$ nm, $W_b = 6.35$ mm, inducing $\sigma_E = 0.098\%$ for 200 m at 77 K. The transverse RW for this vessel, calculated from W_{\parallel} using the Panofsky-Wenzel theorem [20], gives to dipole order, a kick of ≈ 0.27 eV μm^{-1} transversely m^{-1} longitudinally, increasing ϵ by a negligible amount [21]. Finally, the analytic formula [22] and numeric codes [23], which agreed for the parameters considered, were used to calculate a 2.7% increase in ϵ due to 300 μm rms misalignments of the bellows and tapered room to cold transitions of 60 undulator modules.

Extensive magnetic modeling using OPERA 2D and 3D software [24] was performed once the vacuum vessel dimensions were selected. The first results of the modeling demonstrated that to increase B_0 while decreasing λ_u for a fixed W_b the inclusion of iron poles was necessary. Using an iron pole increases the peak field in the conductor, but the current density J required to achieve the same B_0 is reduced. Overall, this gives a better operating margin for the SC; e.g., for $\lambda_u = 14$ mm a B_0 of ~ 0.8 T can be achieved with $J = 400$ Amm^{-2} rather than 1000 Amm^{-2} when iron is not included. The iron poles effectively contribute half the on-axis field. Including iron poles complicates the manufacturing process since initially formers were machined from a single rod of aluminum such that the former and the vacuum vessel were made from one single piece of material. This approach is not possible when iron is used as the vacuum vessel part of the former would shunt the magnetic flux. The geometry of the windings and pole pieces were optimized using computer models. The conclusion of optimizing the geometry was that the device was relatively insensitive to the exact configuration of the wires (e.g., 8 layers of 7 wires or 7 layers of 5 wires, etc.) and the pole dimensions. From the 3D modeling (see Fig. 1), there is a range of undulator parameters (λ_u and W_b) that will all generate 10 MeV circularly polarized photons from a 150 GeV electron beam. From Fig. 1 it can be seen that for $W_b = 6.35$ mm the optimum value of λ_u is 11.5 mm. Therefore, $B_0 = 0.86$ T in order to generate 10 MeV photons with the first harmonic of the radiation spectrum.

In parallel to the wakefield calculations and magnet modeling, several short undulator prototypes were built in order to develop fabrication techniques suitable for producing longer sections for the cryomodule and their performances were confirmed with electrical, mechanical, and magnetic measurements. Issues such as magnetic performance, undulator former accuracy, inclusion of iron poles, incorporating a copper beam vessel into the former, wire insulation, comparison of different wires, the shape of the former groove, developing precise winding and vacuum impregnation techniques, and winding onto a thin walled vessel were all addressed. Winding the undulator with a wire ribbon rather than a single wire significantly reduced technical difficulties encountered at the ends of the

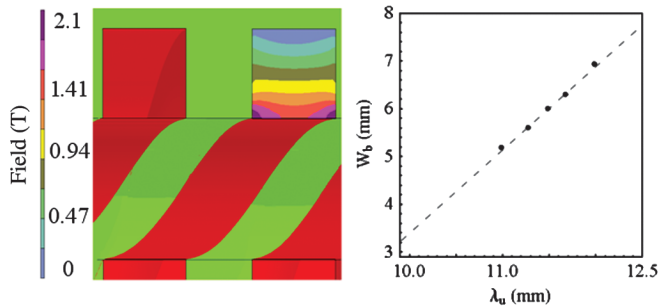


FIG. 1 (color). (Left) Example 3D model showing the field in the winding blocks (red) with an iron former (green). (Right) 3D modeling results of W_b vs λ_u (points) and a line of best fit to the data.

winding and also improved the winding accuracy. The wires were bonded into a flat ribbon that was wound into the former using a bespoke winding machine. To achieve a continuous winding of both helices, sets of pegs at the ends of the undulator were used to reverse the winding direction of the ribbon into the adjacent helical groove. Following winding, the coil was vacuum impregnated with epoxy resin and the wires in the ribbon were interconnected at the terminal block to effectively create a long module excited by one continuous wire. As a result, the completed undulator winding forms a single multilayer, continuous, double helical coil with just two terminations for connection to a power supply. A photograph of a number of the short prototypes is shown in Fig. 2.

After construction of the short prototypes two 1.74 m long undulators were fabricated, M1 and M2, and tested in a vertical test stand before assembly into the 4 m long cryostat (see photograph in Fig. 2). Figure 3 shows the training curves for each magnet, the maximum observed quench current was 301 and 306 A for M1 and M2, respectively (giving an on-axis field of ~ 1.15 T), the operating current for the design field of 0.86 T is $\sim 70\%$ of this, demonstrating a comfortable safety margin. M1 exhibited little quench training but M2 needed extensive quench training; the reason for the difference between

these two undulators is not yet understood and will be the subject of further investigation. The radial component of the magnetic field on the undulator axis was measured by Hall probes at liquid helium temperatures, calibrated by the manufacturer. The setup was similar to that described previously [11] and involved fully immersing each undulator section vertically into a liquid helium bath. Then, two orthogonally aligned Hall probes, H1 and H2, mounted on a graphite push-fit insert were passed through the undulator so that both transverse fields could be measured simultaneously. The probe position was controlled using a stepper motor and screw assembly with a resolution of ± 0.02 mm. The Hall probe voltages were logged using a 16 bit analog-to-digital converter at each point, with typical voltage resolution of ± 0.05 mV. The Hall probe signal at nominal field was ~ 300 mV. In addition to the axial movement the azimuthal position of the probe could be rotated manually to a number of fixed positions which were separated by $90^\circ \pm 0.5^\circ$. The nominal operating current of 216 A (0.86 T) was used for all the measurements. Good agreement was found between the data from H1 and H2 when the transverse Hall effect was taken into account. Transverse first and second field integrals, $I_{x,y}$ and $J_{x,y}$, are given in Table I, where the error is the rms of multiple measurements. As observed in the quench training, there are also differences between M1 and M2 in their integrated magnetic performance. Such differences between nominally identical undulators have been observed before in unshimmed devices [25]. Except at a few points, λ_u and B_0 are consistent to within 1% along the full length of the undulators, this is shown in terms of the undulator K per period in Fig. 3, where $K = \frac{B_0 e \lambda_u}{2 \pi m_e c}$ with c the speed of light and m_e and e the electron mass and charge. The outlying spikes that are at regular ~ 300 mm intervals are attributed to the indexing points used when machining the iron former. As the magnitude of the indexing errors is different for M1 and M2, this at least partially explains why $I_{x,y}$ and $J_{x,y}$ are different. Now that these indexing points have been identified as causing a measurable effect, a more careful procedure will be used in the manufacture of the long

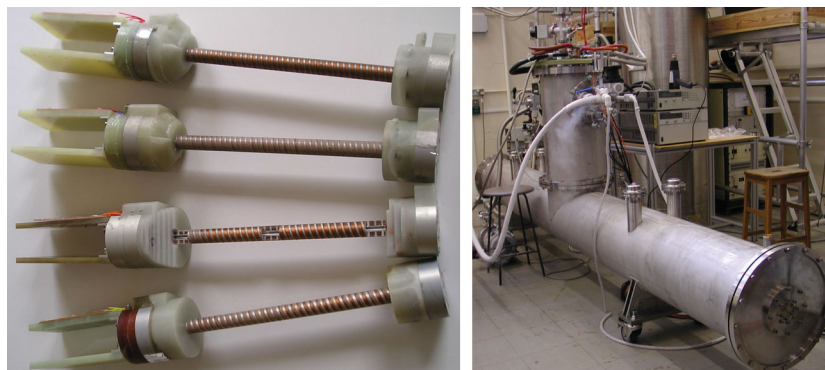


FIG. 2 (color). Photographs of four of the short undulator prototypes (left), 4 m long cryomodule, containing two 1.74 m long undulators, being tested (right).

TABLE I. I (Tmm) and J (Tmm²) field integral data.

Parameter	I_x	I_y	J_x	J_y
M1, H1	-0.49 ± 0.32	-2.19 ± 0.47	-1777 ± 390	-1392 ± 440
M1, H2	-0.73 ± 0.27	-2.13 ± 0.14	-1950 ± 290	-1218 ± 260
M2, H1	0.01 ± 0.11	0.13 ± 0.02	297 ± 11	-1399 ± 90
M2, H2	-0.02 ± 0.07	-0.05 ± 0.13	22 ± 110	-1380 ± 74

formers in the future. A good assessment of the magnetic performance of the device is to calculate the photon and circular polarization (CP) spectrum from an electron passing through the field. The photon output through a 3 mm \times 3 mm aperture 500 m downstream of the cryomodule, the location of the target, is shown in Fig. 3. This is the output of a single electron passing through first the M1 and then the M2 fields. The initial angle and displacement of the electron was optimized to give a straight trajectory through the device. Also shown in Fig. 3 is the result for an ideal helical undulator with similar average K , λ_u , B_0 , and length. Following the magnetic testing, both undulators were incorporated into a single 4 m long cryostat. The cryostat was successfully cooled down and both undulators were powered simultaneously at their operating current for several hours without quenching (Fig. 2).

A fully working high-field, short-period 4 m long prototype SC helical undulator cryomodule suitable for use in a future linear collider e^+ source has been designed, manufactured, and successfully tested; 60 such modules are expected to induce $\sigma_E = 0.098\%$ and increase ϵ by 2.7% for the ILC. The required on-axis peak field of 0.86 T

has been achieved with $\lambda_u = 11.5$ mm, $A_b = 5.85$ mm, $W_b = 6.35$ mm operating at 70% of the quench current, indicating that λ_u could be further reduced at the expense of some of this safety margin. However, a useful test before further reduction of λ_u would be to test the complete cryostat with a real electron beam of ~ 1 GeV. This would allow for measurement of the beam induced heating and would also allow the spectrum to be measured and compared with that predicted from the magnetic measurements. The predicted spectrum compares well with an ideal device indicating that the e^+ yield will be as anticipated. However, the CP rate is somewhat reduced and so further studies will look at the absolute polarization of the e^+ generated and how this compares with the ideal case. Although designed and manufactured to demonstrate the feasibility of such a device for a future linear collider e^+ source, the development of SC undulators suitable for synchrotron and FEL-based light sources is an active area of research with devices becoming operational [26]. Many of the techniques learned are now being applied by the authors to develop SC undulators for light sources.

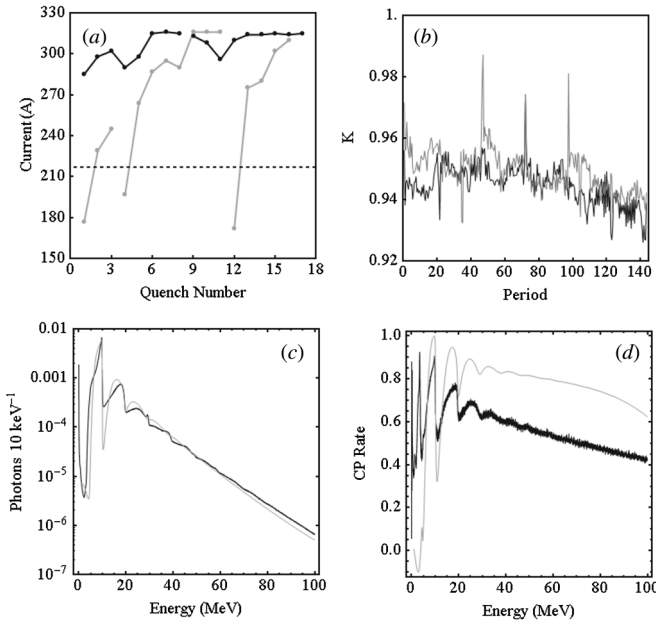


FIG. 3. Training curves (a) and K per period (b) for M1 (black lines) and M2 (gray lines). Number of photons per electron per 10 keV bandwidth (c) and CP rates (d) for measured fields (black lines) and ideal fields (gray lines).

*Also at Fermi National Accelerator Laboratory, P.O. Box 500, Batavia, Illinois 60510, USA.
duncan.scott@stfc.ac.uk

- [1] J.E. Clendenin, in *Proceedings of the 1989 Particle Accelerator Conference, Chicago* (IEEE, Piscataway, NJ, 1989), pp. 1107–1111.
- [2] A. Ushakov *et al.*, in *Proceedings of the European Particle Accelerator Conference, Edinburgh, 2006* [<http://accelconf.web.cern.ch/AccelConf/e06/PAPERS/WEPLS046.PDF>].
- [3] G.A. Moortgat-Pick *et al.*, *Phys. Rep.* **460**, 131 (2008).
- [4] V. Balakin and A. Mikhailichenko, Budker Institute of Nuclear Physics Technical Report No. 79-85, 1979.
- [5] G. Alexander *et al.*, *Phys. Rev. Lett.* **100**, 210801 (2008).
- [6] G. Alexander *et al.*, *Nucl. Instrum. Methods Phys. Res., Sect. A* **610**, 451 (2009).
- [7] T. Okugi *et al.*, *Jpn. J. Appl. Phys.* **35**, 3677 (1996).
- [8] T. Omori *et al.*, *Phys. Rev. Lett.* **96**, 114801 (2006).
- [9] ILC Reference Design Report: Accelerator, edited by N. Phinney *et al.*, 2007, Vol. 3 (ILC-REPORT-2007-001).
- [10] L. Zang *et al.*, in *Proceedings of the 23rd Particle Accelerator Conference, Vancouver, 2009* [<http://accelconf.web.cern.ch/AccelConf/PAC2009/papers/mo6rfp092.pdf>].

- [11] D. J. Scott *et al.*, *Phys. Rev. ST Accel. Beams* **10**, 032401 (2007).
- [12] L. R. Elias and J. M. Madey, *Rev. Sci. Instrum.* **50**, 1335 (1979).
- [13] N. Vinokurov, *Nucl. Instrum. Methods Phys. Res., Sect. A* **246**, 105 (1986).
- [14] K. Flöttmann, Ph.D. thesis, Hamburg University, 1993.
- [15] D. J. Scott, Ph.D. thesis, University of Liverpool, 2008.
- [16] K. L. F. Bane, Report No. SLAC-PUB-10707, 2004.
- [17] D. J. Scott *et al.*, in *Proceedings of the 23rd Particle Accelerator Conference, Vancouver, 2009* [<http://accelconf.web.cern.ch/AccelConf/PAC2009/papers/fr5rfp092.pdf>].
- [18] G. E. H. Reuter and E. H. Sondheimer, *Proc. R. Soc. A* **195**, 336 (1948).
- [19] G. V. Stupakov, *Phys. Rev. ST Accel. Beams* **1**, 064401 (1998).
- [20] W. K. H. Panofsky and W. A. Wenzel, *Rev. Sci. Instrum.* **27**, 967 (1956).
- [21] D. J. Scott and J. Jones, Report No. EUROTeV-Report-2006-007, 2007.
- [22] P. Tenenbaum *et al.*, *Phys. Rev. ST Accel. Beams* **10**, 034401 (2007).
- [23] I. Zagorodnov and T. Weiland, *Phys. Rev. ST Accel. Beams* **8**, 042001 (2005).
- [24] Available from Vector Fields Ltd, Kidlington, Oxford OX5 1JE, UK.
- [25] B. J. A. Shepherd and J. A. Clarke, *Nucl. Instrum. Methods Phys. Res., Sect. A* **654**, 8 (2011).
- [26] S. Casalbuoni *et al.*, *Phys. Rev. ST Accel. Beams* **9**, 010702 (2006).